Technical University of Denmark

DTU

Comparison of fin-and-tube interlaced and face split evaporators with flow mal-distribution and compensation

Kærn, Martin Ryhl; Elmegaard, Brian; Larsen, L.F.S.

Link back to DTU Orbit

DTU Library
Technical Information Center of Denmark

COMPARISON OF FIN-AND-TUBE INTERLACED AND FACE SPLIT EVAPORATORS WITH FLOW MAL-DISTRIBUTION AND COMPENSATION

KÆRN M.R. [(*,**)], **ELMEGAARD B.** [(**)], **LARSEN L.F.S.** [(*)]

[(*)] Danfoss A/S, Refrigeration and Air-Conditioning,
Nordborgvej 81, DK-6430 Nordborg, Denmark,
martin@danfoss.com
[(**)] Technical University of Denmark, Department of Mechanical Engineering,
Nils Koppels Allé Bygn. 403, DK-2800 Lyngby, Denmark,
pmak@mek.dtu.dk

ABSTRACT

Flow mal-distribution in fin-and tube evaporators for residential air-conditioning is investigated by numerical simulation. In particularly, the interlaced and the face split evaporator are compared in flow mal-distribution conditions. The considered sources of mal-distribution are: Liquid/vapor distribution and airflow distribution. Furthermore, compensation of flow mal-distribution by control of individual channel superheat is studied for each type of evaporator. It is shown that the interlaced evaporator is better at flow mal-distribution than the face split evaporator. However, if individual channel superheats are controlled, the face split evaporator achieves the best performance, i.e. an increase of 7% in UA-value and 1.6% to 2.4% in COP compared to the interlaced evaporator without compensation.

1.   INTRODUCTION

For A-shaped fin-and-tube evaporators in residential air-conditioning, the chosen type of circuitry by the manufacturers changed a couple of years ago. It changed from the face split to the interlaced circuitry, see figure 1. The interlaced circuitry shows a significant increase in cooling capacity compared to the face split circuitry. The main reason is the better compensation of flow mal-distribution by design. In the current paper this choice is discussed with regards to further compensation of flow mal-distribution by control of individual channel superheats.

Flow mal-distribution in fin-and-tube evaporators has been shown to decrease the performance of the evaporator and the system both experimentally (Payne and Domanski, 2003) and numerically (Kærn et al., 2011a, Kim et al., 2009b). Both air side and refrigerant side effects may cause flow non-uniformities, e.g. non-uniform airflow, air-temperature, humidity or frost, fouling, two-phase inlet distribution, feeder tube bending and improper heat exchanger design. In this study we only address a non-uniform airflow and a non-uniform liquid/vapor distribution to the evaporator.

Most efforts of compensating flow mal-distribution have been addressed to the design of the evaporator circuitry. Domanski and Yashar (2007) applied a novel optimization system called ISHED (intelligent system for heat exchanger design) to optimize refrigerant circuitry in order to compensate airflow mal-distribution. They measured the air velocity profile using particle image velocimetry (PIV) and used that as input to their numerical model and reported that the cooling capacity was increased by 4.2% compared to an interlaced type of circuitry.

Studies regarding the benefits by control of individual superheat have also been conducted. Payne and Domanski (2003) showed experimentally that performance degradation due to a non-uniform airflow could be recovered to within 2% of the original cooling capacity at uniform airflow conditions. Kim et al. (2009a) studied benefits of upstream vs. downstream control of individual channel superheat on a fin-and-tube five channel R410A heat pump numerically. The study showed that the upstream control outperformed the downstream control. They found that upstream control was able to recover up to 99.9% of the penalties of mal-distribution. Kærn et al. (2011b) also studied compensation by control of individual channel superheat.

Here a recovery of 94.3% in COP was found at a nearly complete air blockage of half of the evaporator, keeping the total air volume flow constant.

To this point no investigation is known to the authors where tube circuitries are compared with flow mal-distribution and compensated by control of individual channel superheat. The objective of this paper is to study the benefits (in UA-value and COP) of compensation by control of individual channel superheats on the interlaced and the face split evaporator. The method of compensation involves a coupled expansion and distributor device marketed as EcoFlow(TM), which is able to distribute the mass flow according to the individual superheat of each channel by only measuring the overall superheat (Funder-Kristensen et al., 2009; Mader and Thybo, 2010). The paper includes a brief description of the numerical model, an analysis of flow mal-distribution in both evaporators and compensation by control of individual channel superheat.
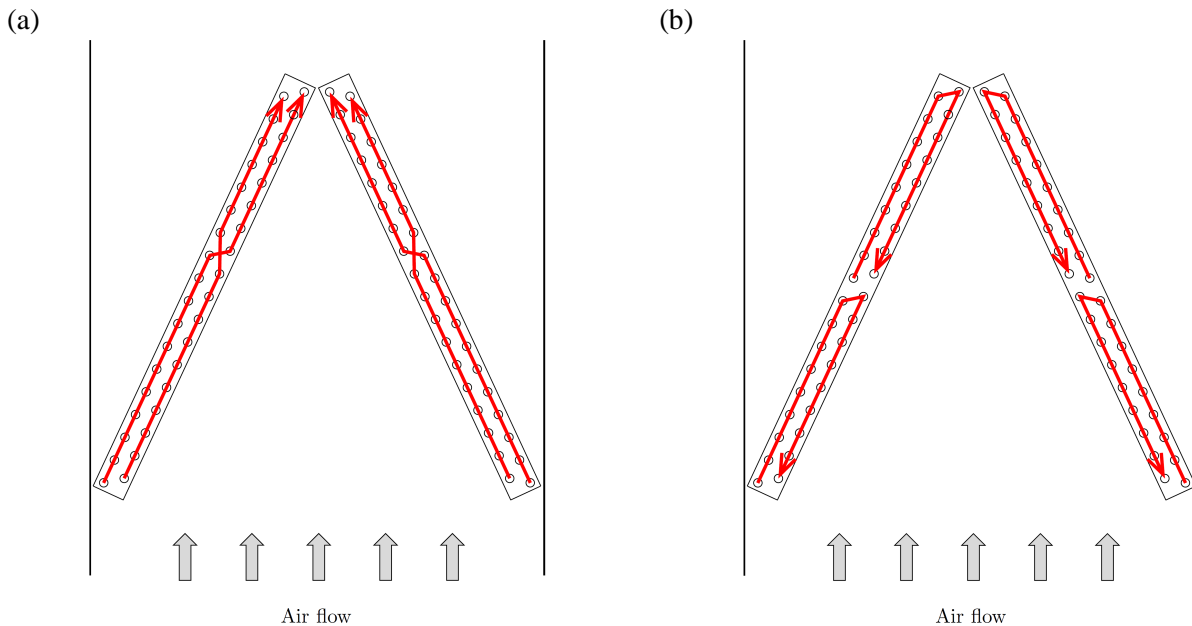
(a)   (b)

Air flow   Air flow

Figure 1. Tube circuitries of (a) the interlaced evaporator and (b) the face split evaporator

2.   SIMULATION MODEL

A model of an 8.8 kW R410A RAC system was developed by Kærn et al. (2011a) in Dymola 7.1, and it has been updated in this study to include the tube circuiting effects of the evaporator. Thermophysical properties for R410A are obtained from the refeqns package (Skovrup, 2009). In order to predict the refrigerant mal-distribution in the evaporator a distributed one-dimensional mixture model was chosen. For the condenser, the simpler moving boundary model of Zhang et al. (2006) was chosen, which averages the vapor, two-phase and liquid regions. Both the evaporator and condenser are dynamic, so that further investigations are possible with regards to the dynamics of the system. Only steady state results are given in this paper. The models of the expansion and compressor are quasi-static. Momentum transfer and frictional pressure drop are only addressed in the evaporator tubes, U-bends and feeder tubes, in order to predict the mass flow distribution in the evaporator.

2.1.   Geometry and correlations
Table 1 shows the main geometry of the test case evaporator and condenser. The tube inner walls are smooth. Furthermore, the feeder tubes to the evaporator have an internal diameter of 3 mm and a length of 300 mm. Note that the coil geometry is the same for both the interlaced and face split evaporator, however the tube connections or circuiting are different as shown on figure 1.

The two coils in the evaporator are assumed to be in similar mal-distribution conditions. In the condenser, refrigerant enters four of the channels and is mixed before entering the fifth channel. Since mal-distribution is not addressed in the condenser, it is assumed to be four straight tubes with no mal-distribution.

Each discrete cell of the evaporator is calculated as a small heat exchanger with uniform transport properties. Mass, momentum and energy conservation equations are applied to the refrigerant in each cell, where homogeneous flow and thermodynamic equilibrium are assumed. Furthermore changes in kinetic and potential energies are neglected. It is assumed that the tube walls have rotational symmetry, i.e. no heat conduction in the azimuthal direction. Mass and energy conservation equations are applied to the air, which is assumed to be dry. Similar assumptions are used in the condenser model of the refrigerant and air-flow, however the heat resistance and the dynamics in the condenser wall are neglected. The used correlations for both the evaporator and the condenser are given in table 2. Furthermore, effectiveness-NTU relations for cross flow heat exchangers are employed.

Table 1: Main geometry of the evaporator and condenser

	Evaporator	Condenser
Number of coils	2	1
Number of channels in each coil	2	5
Number of tubes in each channel	18	6
Tube length [mm]	444.5	2100
Inner tube diameter [mm]	7.6	7.6
Outer tube diameter [mm]	9.6	9.6
Transverse tube pitch [mm]	25.4	25
Longitudinal tube pitch [mm]	21.25	
Fins	Louvred	Louvred
Fin pitch [mm]	1.81	1.15
Total outside area [m^2]	19.2	52.2
Number of cells per tube	3	

Table 2: Overview of used correlations

Air-side	
Heat transfer	Wang et al. (1999)
Fin efficiency	Schmidt (1949) (Schmidt approximation)
Single phase	
Heat transfer	Gnielinski (1976)
Friction (evaporator)	Blasius (2002)
Bend friction (evaporator)	Ito (1960)
Two-phase	
Heat transfer (evaporator)	Shah (1982)
Heat transfer (condenser)	Shah (1979)
Friction (evaporator)	Müller-Steinhagen and Heck (1986)
Bend friction (evaporator)	Geary (1975)

The expansion valve is modeled as an isenthalpic process and it essentially controls the superheat out of the evaporator manifold by the mass flow rate through the valve. The manifold is modeled by mixing of the refrigerant streams, i.e. mass and energy conservation equations are applied. The geometric volume flow of the compressor is 6.239 m^{3}h^{-1}, and polynomials from the rating of the compressor are used to compute the isentropic and volumetric efficiencies.

2.2. Distribution parameters
To study the effect of inlet liquid/vapor phase distributions and non-uniform airflow distributions, we have defined two distribution parameters. The phase distribution parameter, F_x, is defined by

$$F_x = \frac{x_2}{x_{in}}$$ (1)

where
x_{in} = entering vapor quality to the distributor [-], x_2 = entering vapor quality to channel 2 [-].

When F_x is unity, the vapor quality into the channels is equal. When F_x is zero, only liquid is fed into channel 2. Mass and energy conservation equations are applied to compute the vapor quality into channel 1. The numbering of the channels for both the interlaced and the face split are shown on figure 2a. The airflow distribution parameter, F_{air}, is defined by

$$V(y) = V_m F_{air} + y \frac{2V_m(1-F_{air})}{L_t} \tag{2}$$

where
V_m = mean frontal velocity [m/s], y = transverse coordinate [m], L_t = transverse length of the coil [m].
When F_{air} is unity, the airflow profile is uniform across the coil. When F_{air} is zero, the airflow profile becomes the worst possible linear one-dimensional profile in the transverse direction, see figure 2b.
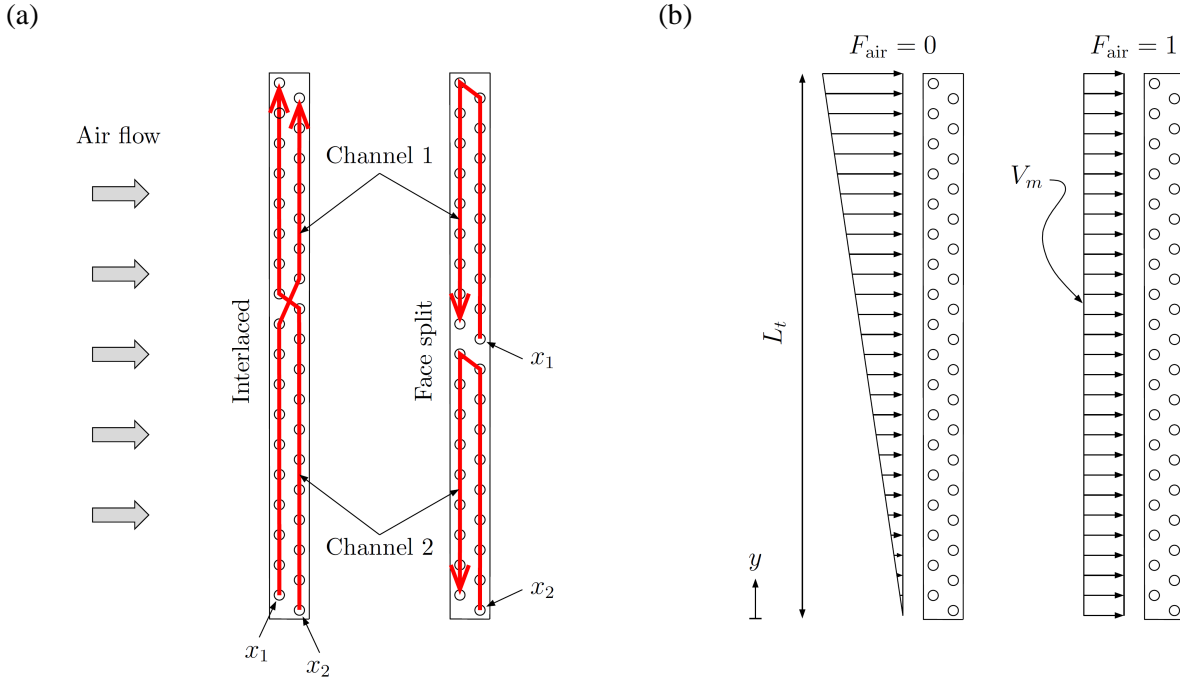

Figure 2. (a) channel numbering for each evaporator and (b) one-dimensional airflow profiles

2.3.   Boundary conditions
In the system model the overall superheat is kept at 5 K. When compensating, the expansion device controls both channel superheats to 5 K. During start-up of the simulation at no mal-distribution the charge of the system is determined, so that the subcooling becomes 2 K. Then the different distribution parameters are varied individually and each steady state result is obtained. The indoor and outdoor air temperatures are 26.7°C and 35°C, respectively. The mean frontal air velocities are 1.16 and 0.68 m s^{-1} to the evaporator and condenser, respectively.

3.   RESULTS

In this section the results of the simulations of flow mal-distribution are presented for each circuitry type, i.e. the interlaced and the face split evaporator. The distribution parameters are varied individually from 1 to 0, imposing an increasing degree of mal-distribution. Firstly, we considered the cases without compensation and, secondly, we consider the case with compensation by control of individual superheat.

3.1.   Mal-distribution from the distributor without compensation
The distribution of refrigerant mass flux as function of the phase distribution parameter is shown on figure 3a for each coil of the evaporators. It shows that the mass flux distribution is dependent on F_x, so that more mass comes through the channel with lower inlet vapor quality (channel 2) and less mass comes through the channel with higher inlet vapor quality (channel 1). This is determined by the pressure drop across the channels that must be equal. Indeed more mass will travel through the channel with lower vapor quality,

since the pressure drop of the liquid phase is lower than the pressure drop of the vapor phase. At no mal-distribution ($F_x = 1$) the face split evaporator shows higher mass fluxes for both channels indicating a higher cooling capacity, however they decrease at higher mal-distribution and become lower than the interlaced evaporator at $F_x = 0.55$.
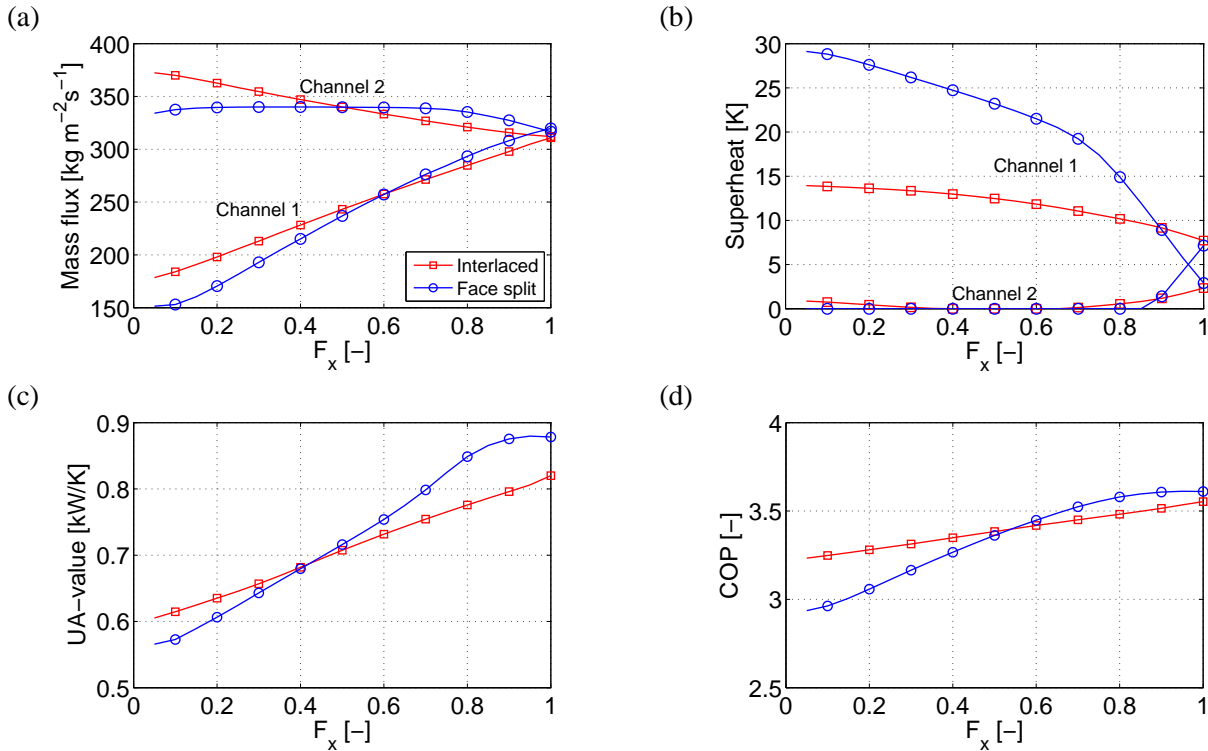

Figure 3. Selected parameters vs. the phase distribution parameter

The consequence of the refrigerant mal-distribution is seen in figure 3b, which shows the individual channel superheats for each coil of the evaporators. At $F_x = 0.85$, liquid is flowing out of channel 2 for the face split evaporator. This point is important because the two-phase area of the face split evaporator decreases, when full evaporation is not reached in channel 2. A larger superheated area in channel 1 is required in order to evaporate this surplus liquid, thus the overall UA-value decreases as seen on figure 3c. The interlaced evaporator does not experience the same degree of superheat non-uniformity, and it therefore has a smaller reduction in the overall UA-value as F_x decreases. However, the face split evaporator performs better at low mal-distribution. This is because of the tube circuitry. The two channels of the face split evaporator are counter-cross flow, however the interlaced is both counter-cross flow (channel 2) and parallel-cross flow (channel 1). When constructing a heat exchanger it should always be attempted to use the temperature potential between the heat exchanging fluids in the best possible way. It is not the case when the superheated regions, which have lower UA-value, are aligned next to each other in the flow direction, as for the interlaced evaporator. There is a higher temperature potential for heat transfer in both the superheated regions of the face split evaporator, since they are aligned in the first tube row. In turn, the face split evaporator will minimize the superheated region, since the gradient of the refrigerant vapor is higher than for the interlaced evaporator.

The COP of the RAC systems (figure 3d) is affected in similar manner as the UA-value, however not as dramatic. The tradeoff between the face split and the interlaced evaporator is at $F_x = 0.55$ for the current systems.

3.2. Mal-distribution from the airflow without compensation
The distribution of refrigerant mass flux as function of the airflow distribution parameter is shown on figure 4a for each coil of the evaporators. For the face split evaporator, the refrigerant mass flux distribution is almost equal in each channel as F_{air} decreases. For the interlaced evaporator there is some divergence. The mass fluxes are again higher for the face split evaporator at low mal-distribution indicating a higher cooling

capacity and performance. However, the mass fluxes of the face split evaporator decrease even more than the interlaced evaporator at higher mal-distribution.
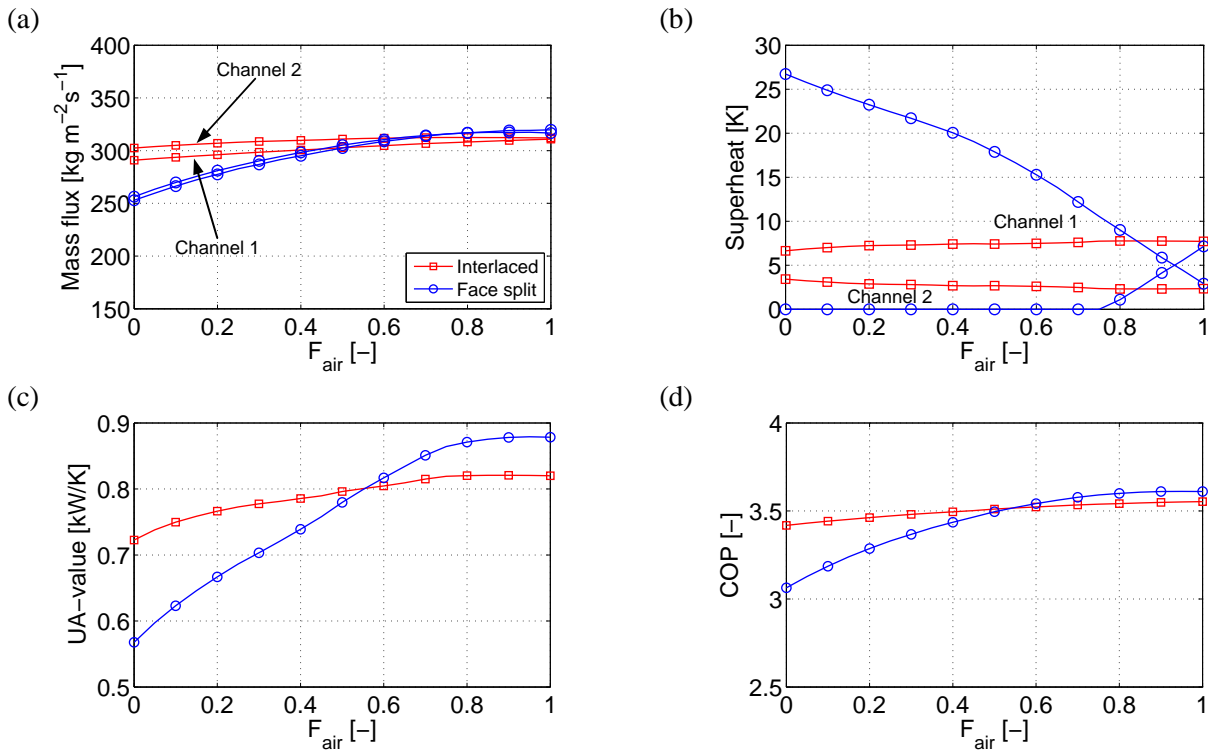

Figure 4. Selected parameters vs. the airflow distribution parameter

Figure 4b shows the corresponding superheat of each channel in the coils of both evaporators. It is seen that the interlaced evaporator recovers the airflow mal-distribution quite well, i.e. the superheated region of the evaporator is not increased. This is in contrast to the face split evaporator, which shows that liquid comes out of channel 2 at $F_{air} = 0.75$, thus the superheat of channel 1 increases in order to ensure an overall superheat of 5 K.

Despite the interlaced superior mal-distribution recovery, the face split evaporator performs better at $F_{air} > 0.55$ and $F_x > 0.55$ in terms of overall UA-value and COP, see figure 3c, 3d, 4c and 4d. As mentioned in the previous section, this is because the superheated regions with low UA-value are placed in the first row of the coils in the face split evaporator, where the temperature driving potential is highest. It seems a coincidence that the trade-off value is 0.55 for both F_{air} and F_x, however, the trade-off is subject to their definitions by equation 1 and 2. The reason why the interlaced evaporator is used today seems because of the flow mal-distribution, which is better recovered by the interlaced evaporator.

3.3. Compensation by control of individual superheat
The method of compensation involves a coupled expansion and distributor device, which is able to distribute the mass flow according to the individual superheat of each channel by only measuring the overall superheat (Funder-Kristensen et al., 2009; Mader and Thybo, 2010). The distribution occurs before the expansion, and the actual expansion is occurring into the individual feeder tubes. Thus the liquid/vapor phase cannot be mal-distributed. The expansion device is distributing the liquid and vapor phases uniformly. Moreover, the inlet specific enthalpy to each channel is the same, and the expansion device already compensates the liquid/vapor mal-distribution. Thus, in this section we only vary the airflow distribution parameter. By allowing the individual mass flows to be controlled, the pressure drop through each channel is not necessarily equal. Therefore, an additional inlet pressure difference is allowed in the model.

The control of the individual channel superheat eliminates the different superheated regions in both evaporators. The elimination of the superheated region is however higher for the face split evaporator, as indicated on figure 4b, since the interlaced already by design compensates air-flow mal-distribution to some extend. The result is an increased overall UA-value and COP as depicted on figure 5a and 5b.

Despite the better performance of the interlaced evaporator with compensation, it does not perform better than the face split evaporator without compensation at $F_{air} > 0.65$. The face split evaporator with compensation performs the best at all values of F_{air}. Both evaporators experience a better performance when controlling the individual superheat. Interestingly, the difference in COP between the two evaporators with compensation is increasing slightly as F_{air} decreases.
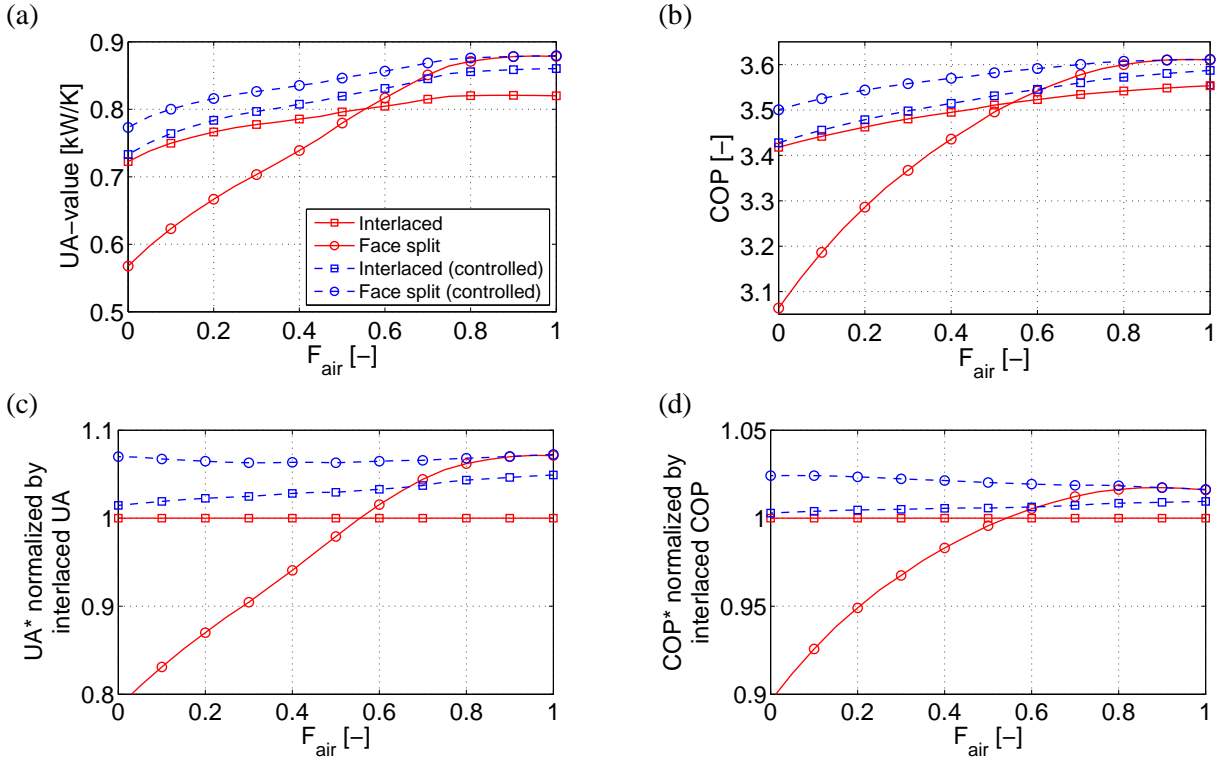

Figure 5. Comparison of UA-value and COP with/without compensation of airflow mal-distribution

If we normalize the results from figure 5a and 5b with the current evaporator used today, i.e. the interlaced without individual superheat control, we see the actual increase when applying the control of individual superheat to each evaporator as function of F_{air}, as depicted on figure 5c and 5d. For the face split with compensation, this increase in UA-value stays around 7% as F_{air} decreases, however, the interlaced with compensation shows a decrease from 4.9% to 1.5%. The increase in COP increases from 1.6% to 2.4% for the face split evaporator with compensation as F_{air} decreases, however, the interlaced evaporator with compensation shows a decrease from 1.0% to 0.3%.

4.   DISCUSSION

The benefits shown in section 3.3 are at compensation for similar airflow mal-distribution in each coil. However, there could also be coil to coil airflow mal-distribution. There could also be non-uniform liquid/vapor distribution in the distributor as addressed in section 3.1 or other kinds of mal-distribution e.g. fouling. These issues would contribute to the total degradation of flow mal-distribution. Thus higher benefits are expected in practice than showed in section 3.3, when applying the control of individual channel superheat.

5.   CONCLUSION

We conclude that at uniform flow conditions, it is always better to place the superheated regions with low UA-value in the first row of the coils, where the temperature driving potential is highest, as done in the face split evaporator. However, since we may have flow mal-distribution in the evaporator, the interlaced evaporator is however the preferred evaporator today. If the flow mal-distribution is controllable in a way that is independent of circuitry, as done in section 3.3, then the face split circuitry will give the best

performance. Furthermore, an increase in the number of rows in larger coils is expected to contribute to the difference between the performance of the face split and interlaced evaporator with compensation.

Compared to the interlaced evaporator without compensation, the increase by using the face split evaporator with compensation is 7% in UA-value and 1.6% to 2.4% in COP.

6. REFERENCES

Blasius, P. R. H., 2002. *VDI Wärmeatlas*, 9th Edition. Springer-Verlag, Ch. Lab.

Domanski, P. A., Yashar, D., 2007. Application of an evolution program for refrigerant circuitry optimization. *Proc. ACRECONF "Challenges To Sustainability"*. New Delhi, India.

Dymola 7.1, 2008. *Dynamic Modeling Laboratory, Dymola User's Manual*, version 7.1. Dynasim AB, Research Park Ideon SE-223 70, Lund, Sweden.

Funder-Kristensen, T., Nicolaisen, H., Holst, J., Rasmussen, M. H., Nissen, J. H., 2009. Refrigeration system. US Patent, Pub. No.: US 2009/0217687 A1.

Geary, D., 1975. Return bend pressure drop in refrigeration systems. *ASHRAE Trans.* 81, 250–264.

Gnielinski, V., 1976. New equation for heat and mass transfer in turbulent pipe and channel flow. *Int. Chem. Eng.* 16, 359–368.

Ito, H., 1960. Pressure losses in smooth pipe bends. *Trans. ASME, J. Basic Engineering* 82, 131–143.

Kim, J.-H., Braun, J., Groll, E., 2009a. Evaluation of a hybrid method for refrigerant flow balancing in multi-circuit evaporators. *Int. J. Refrigeration* 32, 1283–1292.

Kim, J.-H., Braun, J., Groll, E., 2009b. A hybrid method for refrigerant flow balancing in multi-circuit evaporators: Upstream versus downstream flow control. *Int. J. Refrigeration* 32, 1271–1282.

Kærn, M. R., Brix, W., Elmegaard, B., Larsen, L. F. S., 2011a. Performance of residential air-conditioning systems with flow maldistribution in fin-and-tube evaporators. International Journal of Refrigeration, 34, 696-706.

Kærn, M. R., Brix, W., Elmegaard, B., Larsen, L. F. S., 2011b. Compensation of flow maldistribution in fin-and-tube evaporators for residential air-conditioning. International Journal of Refrigeration, In Press, Accepted Manuscript.

Payne, W. V., Domanski, P. A., 2003. Potential benefits of smart refrigerant distributors. *Air-Conditioning and Refrigeration Technology Institute*, Arlington, VA, USA.

Mader, G., Thybo, C., 2010. An electronic expansion valve with automatic refrigerant distribution control. In: Deutsche Kälte-Klima-Tagung. Magdeburg, Germany.

Müller-Steinhagen, H., Heck, K., 1986. A simple friction pressure drop correlation for two-phase flow in pipes. *Chem. Eng. Proc.* 20, 297–308.

Schmidt, T. E., 1949. Heat transfer calculations for extended surfaces. *Ref. Eng.*, 351–357.

Shah, M. M., 1979. A general correlation for heat transfer during film condensation inside pipes. *Int. J. Heat and Mass Transfer* 22, 547–556.

Shah, M. M., 1982. Chart correlation for saturated boiling heat transfer: Equations and further study. *ASHRAE Trans.* 88, 185–196.

Skovrup, M. J., 2010. Thermodynamic and thermophysical properties of refrigerants. Department of Energy Engineering, Technical University of Denmark.

Wang, C.-C., Lee, C.-J., Chang, C.-T., Lin, S.-P., 1999. Heat transfer and friction correlation for compact louvered fin-and-tube heat exchangers. *Int. J. Heat and Mass Transfer* 42, 1945–1956.

Zhang, W.-J., Zhang, C.-L., 2006. A generalized moving-boundary model for transient simulation of dry-expansion evaporators under larger disturbances. *Int. J. Refrigeration* 29, 1119–1127.